

Synthesis of strong SiV photoluminescent diamond particles on silica optical fiber by chemical vapor deposition

Zongchun Yang(仰宗春), Yingshuang Mei(梅盈爽), Chengke Chen(陈成克), Yinlan Ruan(阮银兰), Xiaojun Hu(胡晓君)
Citation: Chin. Phys. B . 2018, 27(3): 038101. **doi:** 10.1088/1674-1056/27/3/038101

Journal homepage: http://cpb.iphy.ac.cn; http://iopscience.iop.org/cpb
What follows is a list of articles you may be interested in

Synthesis of diamonds in Fe—C systems using nitrogen and hydrogen co-doped impurities under HPHT

Shi-Shuai Sun(孙士帅), Zhi-Hui Xu(徐智慧), Wen Cui(崔雯), Xiao-Peng Jia(贾晓鹏), Hong-An Ma(马红安)
Chin. Phys. B . 2017, 26(9): 098101. **doi:** 10.1088/1674-1056/26/9/098101

Different effect of NiMnCo or FeNiCo on the growth of type-IIa large diamonds with Ti/Cu as nitrogen getter

Shang-Sheng Li(李尚升), He Zhang(张贺), Tai-Chao Su(宿太超), Qiang Hu(胡强), Mei-Hua Hu(胡美华), Chun-Sheng Gong(龚春生), Hon-An Ma(马红安), Xiao-Peng Jia(贾晓鹏), Yong Li(李勇)
Chin. Phys. B . 2017, 26(6): 068102. **doi:** 10.1088/1674-1056/26/6/068102

Synthesis of N-type semiconductor diamonds with sulfur, boron co-doping in FeNiMnCo-C system at high pressure and high temperature

He Zhang(张贺), Shangsheng Li(李尚升), Taichao Su(宿太超), Meihua Hu(胡美华), Hongan Ma(马红安), Xiaopeng Jia(贾晓鹏), Yong Li(李勇)
Chin. Phys. B . 2017, 26(5): 058102. **doi:** 10.1088/1674-1056/26/5/058102

High thermal stability of diamond-cBN-B_4C-Si composites

Hong-Sheng Jia(贾洪声), Pin-Wen Zhu(朱品文), Hao Ye(叶灏), Bin Zuo(左斌), Yuan-Long E(鄂元龙), Shi-Chong Xu(徐仕翀), Ji Li(李季), Hai-Bo Li(李海波), Xiao-Peng Jia(贾晓鹏), Hong-An Ma(马红安)
Chin. Phys. B . 2017, 26(1): 018102. **doi:** 10.1088/1674-1056/26/1/018102

Large single crystal diamond grown in FeNiMnCo-S-C system under high pressure and high temperature conditions

He Zhang(张贺), Shangsheng Li(李尚升), Taichao Su(宿太超), Meihua Hu(胡美华), Guanghui Li(李光辉), Hongan Ma(马红安), Xiaopeng Jia(贾晓鹏)
Chin. Phys. B . 2016, 25(11): 118104. **doi:** 10.1088/1674-1056/25/11/118104

Synthesis of strong SiV photoluminescent diamond particles on silica optical fiber by chemical vapor deposition*

Zongchun Yang(仰宗春)[1], Yingshuang Mei(梅盈爽)[1], Chengke Chen(陈成克)[1], Yinlan Ruan(阮银兰)[2], and Xiaojun Hu(胡晓君)[1,†]

[1] College of Materials Science and Engineering, Zhejiang University of Technology, Hangzhou 310014, China
[2] ARC Centre of Excellence in Nanoscale Biophotonics, Institute of Photonics and Advanced Sensing, The University of Adelaide, Adelaide, SA 5005, Australia

(Received 9 September 2017; revised manuscript received 12 December 2017; published online 11 February 2018)

The separated silicon-vacancy (SiV) photoluminescent diamond particles were synthesized on a silica optical fiber by hot filament chemical vapor deposition (HFCVD). The effects of the pre-treated method and chamber pressure on the microstructure and photoluminescence of the diamond particles were investigated. The results show that the diamond particles are homogeneously distributed on the surface of the optical fiber. With the chamber pressure increasing from 1.6 kPa to 3.5 kPa, the shape of the particles transforms from flake to circle, while the diamond particles cannot be deposited on the fiber with the pressure further increased to 4.5 kPa. The samples synthesized under 2.5 kPa chamber pressure are composed of diamond particles with size around 200–400 nm, exhibiting stronger SiV photoluminescence with the width of around 6 nm.

Keywords: diamond, silicon vacancy, photoluminescence, optical fiber

PACS: 81.05.uj, 78.55.–m, 51.70.+f **DOI:** 10.1088/1674-1056/27/3/038101

1. Introduction

Single photon source is critical for quantum information processing and quantum communication.[1] The ideal single photon source generates exactly one photon at a time and all photons are identical. As a result, if any two photons were sent through separated arms of a beam-splitter, they can produce full interference. For the application in quantum communication, the most widely used single photon source is generated with nonlinear optics or emitted by two-level systems such as quantum dot and color centers in diamond. The nonlinear optics is not a "real" single photon source which follows the Poisson distribution.[2] The quantum dot such as InAs quantum dot only works well under 10 K.[3] Color centers in diamond such as nitrogen vacancy (NV) center,[4,5] nickel-nitrogen (NE8) center,[6] Cr-related center,[7] and silicon vacancy (SiV) center[8–10] are highly photostable at room temperature.

The single photon source is generally obtained by coupling single photons into optical fibers, which is compatible with the current fiber communication network. There are various methods to achieve this integration of a single photon source with an optical fiber. Schroder *et al.*[11] picked the NV center containing diamond particles onto the optical fiber through the atomic force microscope (AFM) cantilever tip. Ruan *et al.*[12] directly doped the NV diamonds into the tellurite glass, which had a potentially high collection efficiency but increased the risk of damaging the color centers. Rabeau *et al.*[13] directly deposited NV diamond particles on the fiber endface and achieved fluorescence waveguiding. Besides that, scientists[14,15] also integrated the CdSe colloidal quantum dots with a microfiber and achieved a single photon waveguide.

The SiV center in diamond exhibits many extraordinary photon properties, such as high degree of photons polarization and short life time.[16] Recent work indicated that the single SiV center exhibited very high fluorescence counts, suggesting that it could be an efficient photon source for quantum communication application.[17] Kunuku *et al.*[18] prepared ultra-nanocrystalline diamond particles with the size of about 1 μm with SiV fluorescence, which formed nearly continuous films on a soda-lime glass fiber by using a microwave plasma chemical vapor deposition (MPCVD) method. The samples exhibited a relatively strong intensity of SiV fluorescence but a wide zero photon line of about 9.4 nm width. To realize the possibility of coupling single photons of the SiV diamonds into the optical fiber, separated diamond particles deposited on the fiber surface are required.

In this paper, we prepare individual diamond particles on the surface of the fibers and investigate the impact of

*Project supported by the National Natural Science Foundation of China (Grant Nos. 50972129 and 50602039), the International Science Technology Cooperation Program of China (Grant No. 2014DFR51160), the National Key Research and Development Program of China (Grant No. 2016YFE0133200), European Union's Horizon 2020 Research and Innovation Staff Exchange (RISE) Scheme (Grant No. 734578), and the One Belt and One Road International Cooperation Project from Key Research and Development Program of Zhejiang Province, China (Grant No. 2018C04021).

†Corresponding author. E-mail: huxj@zjut.edu.cn

© 2018 Chinese Physical Society and IOP Publishing Ltd

the deposition conditions on the photoluminescence and microstructural properties of the diamond particles. Seeding is a key parameter[19,20] that can strongly affect the diamond CVD growth process on various substrates.[20,21] The dip-coating[22] by low concentration nanodiamond suspension is used to coat individual diamond nanoparticles onto the fiber surface. The effects of different seeding time on the structural and photoluminescent properties of the diamond particles are discussed. In addition, the chamber pressure is found to be another important parameter for the growth of the diamond particles and fabrication of SiV center, while there are few reports about the related studies.

In this paper, the effects of the pre-treatment method and chamber pressure on the diamond quality and SiV photoluminescent property are well studied. The results show that a chamber pressure of 2.5 kPa is superior for the growth of SiV photoluminescent diamond particles with size around 200–400 nm, exhibiting stronger SiV photoluminescence with the width of around 6 nm.

2. Experiment methods

The standard silica single mode optical fiber with the polymer protection etched away in nitric acid was selected in the experiments. The fiber was 2-cm-long with a diameter about 125 μm. The fiber was dipped in acetone and deionized water for 5 min respectively to remove the remaining acid. After cleaning, the optical fiber was seeded with nanodiamond in diamond/polyvinyl alcohol (PVA) & dimethyl sulfoxide (DMSO) solution to improve the diamond nucleation rates. The solution was prepared in two steps. First, 0.2 g PVA was dissolved in 20 g DMSO while ultrasonic was carried out in 80 °C water. After the PVA/DMSO dropwise cooled to room temperature, 0.1 g nanodiamond powder (average size around 100 nm) was added to form the seeding slurry. The seeding time was set as 0, 2 min, 5 min, and 15 min, named as T0, T2, T5, and T15, respectively. After that, the optical fiber was cleaned in deionized water and acetone before being loaded into the reaction chamber.

The diamond particles were synthesized using a hot filament chemical vapor deposition (HFCVD) system. The filament power was kept at 1.7 kW, the relative concentration ratio of components in the gas mixture was acetone: hydrogen = 1:5. The pressure of the gas mixture in the reaction chamber was set as 1.6 kPa, 2.5 kPa, 3.5 kPa, and 4.5 kPa, respectively. The deposition time was fixed to 20 min according to our previous study. The efficient creation of SiV centers is attributed to the plasma etching of the fiber substrate.

Scanning electron microscopy (SEM) (TESCAN VAGA3) measurements were performed to investigate the morphology of the diamond particles on the fiber surface. Their microstructure and composition were examined by visible Raman spectroscopy. The presence of the SiV photoluminescence (PL) on the diamond endface was confirmed using PL spectroscopy. Raman and PL spectra of the diamond particles were collected on the deposition side using a Raman/PL spectrometer (HORIBA HR800) with 514 nm excitation laser.

3. Results and discussion

Figure 1 shows the surface morphology of the diamond particles synthesized on the fiber surface under 1.6 kPa chamber pressure after different seeding time of 0, 2 min, 5 min, and 15 min, which are named as 1.6T0, 1.6T2, 1.6T5, and 1.6T15, respectively. For the sample without seeding, the SEM graph indicates that there is only the contamination on the fiber surface. The SEM graphs also exhibit that flake-shape structures appear for all the seeded samples, and the flake-shape particles with inhomogeneous size are disorderly distributed on the fiber surface. With seeding time extending to 15 min, the flakes tend to connect with each other and form a continuous diamond film. It is indicated that the seeding time of 2 min is appropriate to prepare the separated particles in the case of 1.6 kPa chamber pressure.

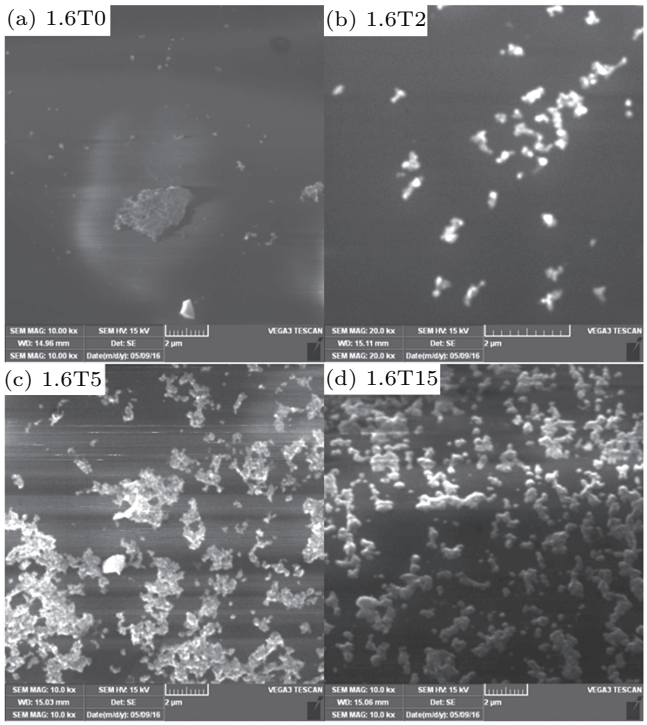


Fig. 1. SEM graphs of diamond particles on fiber surface with different seeding time of 0, 2 min, 5 min, and 15 min under the same chamber pressure of 1.6 kPa and deposition time of 20 min, which are named 1.6T0, 1.6T2, 1.6T5, and 1.6T15, respectively.

Figure 2(a) shows the PL spectra of diamond particles deposited under 1.6 kPa after different seeding time. The SiV photoluminescent peak is not observed in the PL spectra of

1.6T0 and 1.6T2 seeded samples. There is a relatively weak SiV photoluminescence peak appeared at about 738 nm in the PL spectra of the samples 1.6T5 and 1.6T15. The position of SiV zero photon line (ZPL) is at 738.7 nm, which is slightly red-shifted compared to the ideal SiV center ZPL. The full width at half maximum (FWHM) of the SiV ZPL is about 9 nm at room temperature. The intensity ratio of the SiV ZPL to the peak at 552 nm (diamond Raman signal) characterizes the normalized intensity of the SiV ZPL. The normalized intensities of the SiV ZPL are 0.52 and 0.35 for samples 1.6T5 and 1.6T15, respectively. This suggests that sample 1.6T5 has stronger SiV ZPL intensity.

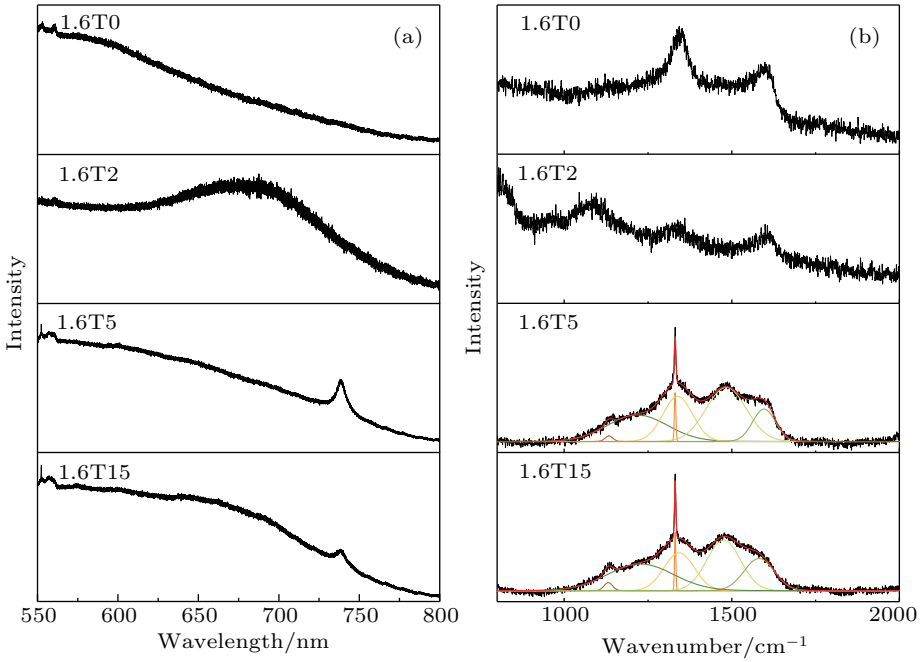


Fig. 2. (color online) (a) PL and (b) Raman spectra of samples 1.6T0, 1.6T2, 1.6T5, and 1.6T15.

The corresponding visible Raman spectra were collected to analyze the composition of the samples at room temperature and fitted with six Gaussian peaks, as shown in Fig. 2(b). The Raman spectra show that the samples 1.6T0 and 1.6T2 exhibit high contents of graphite and amorphous carbon, while no diamond phase is observed. This suggests that a short seeding time causes low nucleation rates, leading to poor diamond quality and the absence of SiV photoluminescence. The samples 1.6T5 and 1.6T15 display a strong diamond peak at about 1330 cm^{-1}, which is slightly blue shifted about 2 cm^{-1} compared with the ideal diamond peak in the Raman spectrum. The fitted diamond contents calculated by using the equation in reference[9,23] are 74% and 76% for samples 1.6T5 and 1.6T15, respectively. The peaks at about 1140 cm^{-1} and 1470 cm^{-1} are due to the reflection of the trans-polyacetylene (TPA),[24–27] which is related to hydrogen in amorphous carbon grain boundaries (GBs) of the diamond particles. The Raman spectra have two large bands at 1350 cm^{-1} and 1560 cm^{-1} (D and G peaks) attributed to sp^2-bonded carbon,[28,29] the G peak is related to graphite specifically. The fitted TPA contents are 9.6% and 7.4% for samples 1.6T5 and 1.6T15, respectively.

Comparing the PL and Raman spectra of samples 1.6T5 and 1.6T15, we find that these samples have a strong diamond peak, but weak SiV ZPL. The Raman spectra indicate that the samples synthesized under 1.6 kPa mainly consist of TPA, graphite, and diamond, thus forming a flake-shape structure, as shown in the SEM morphology. The high content of TPA, which is related to hydrogen in amorphous carbon GBs, quenches the SiV luminescence.[9] Besides that, the existence of graphite has a major influence on the photoluminescence. For the NV center in diamond, it was proved that there exists an energy transfer from the NV center to the graphene monolayer, which results in weaker fluorescence.[30] Here, the graphite contents of samples 1.6T5 and 1.6T15 are 13.5% and 4.1%, which significantly decrease the photoluminescence intensity of SiV.

To decrease the contents of the amorphous carbon and TPA in the particles, we increased the chamber pressure to 2.5 kPa. Figure 3 shows the surface morphologies of the diamond particles synthesized on the surface of the fiber under 2.5 kPa with 20 min deposition time. Their seeding time is 0, 2 min, 5 min, and 15 min, respectively, which are named as 2.5T0, 2.5T2, 2.5T5, and 2.5T15. For the sample 2.5T0, the SEM graph indicates that there is only contamination on the fiber surface. For the samples 2.5T2, 2.5T5, and 2.5T15, the

diamond particles are round shaped with size 200–400 nm. The well-separated diamond particles are obtained with the seeding time of 2 min and 5 min. Comparing to the morphology of the samples synthesized under 1.6 kPa in Fig. 1, we find that the synthesized diamond particles are more homogenously distributed on the fiber under 2.5 kPa.

Figure 4(a) shows the PL spectra of the samples synthesized under 2.5 kPa with different seeding time. The samples exhibit stronger SiV ZPL except for the sample without nanodiamond seeding. The normalized intensities of the SiV ZPL are 2.8, 1.6, and 1.3 for the samples 2.5T2, 2.5T5, and 2.5T15, respectively. Comparing with the samples synthesized under 1.6 kPa, we find that the chamber pressure of 2.5 kPa improves the SiV PL intensity of the diamond particles. The SiV ZPL positions for all samples are red-shifted from the theoretical SiV ZPL position (738 nm) by less than 1 nm, which indicates the existence of internal lattice stress and the surrounding components like graphite and TPA.[24,25] The FWHM of the SiV ZPL is around 5.8–8 nm at room temperature. Thus, higher chamber pressure enhances the number of the SiV centers and decreases the FWHM of the SiV ZPL.

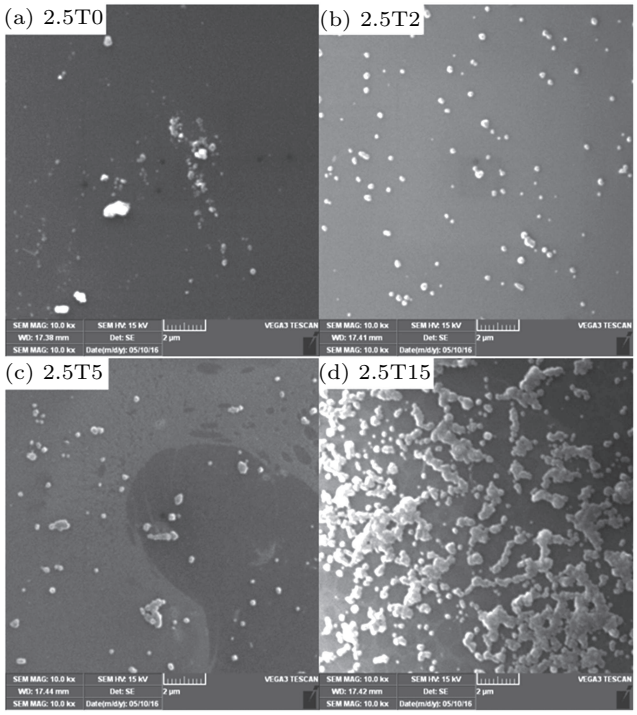


Fig. 3. SEM graphs of diamond particles on the fiber surface with different seeding time of 0, 2 min, 5 min, and 15 min under the same chamber pressure of 2.5 kPa and deposition time of 20 min, which are named 2.5T0, 2.5T2, 2.5T5, and 2.5T15, respectively.

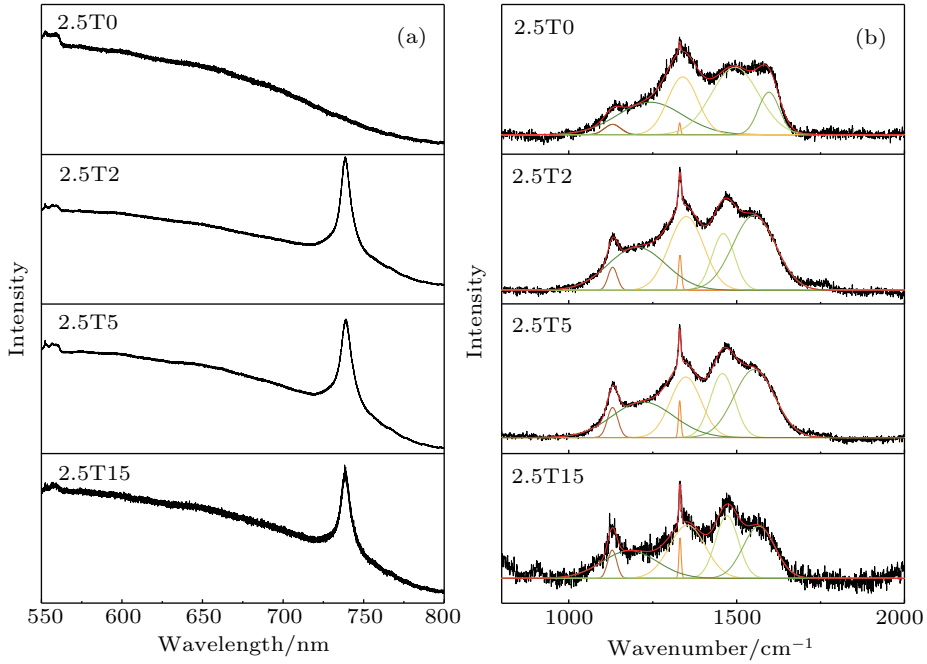


Fig. 4. (color online) (a) PL and (b) Raman spectra of samples 2.5T0, 2.5T2, 2.5T5, and 2.5T15.

Figure 4(b) shows the corresponding Raman spectra of the samples seeded with different time under 2.5 kPa. The Raman spectra indicate that all samples have a weak diamond peak at 1332 cm^{-1} and two TPA peaks at 1140 cm^{-1} and 1470 cm^{-1}. Compared with the Raman spectra in Figs. 2(a) and 4(a), we find that the samples synthesized under different chamber pressures exhibit different diamond compositions. The diamond contents are 40.3%, 72%, 71%, and 76% with the TPA contents of 24.7%, 4.3%, 6.3%, and 6.0% for the samples 2.5T0, 2.5T2, 2.5T5, and 2.5T15, respectively, indicating a massive non-diamond phase in the samples without SiV peaks. These contents cover the diamond grains, thus quenching the excitation of SiV photon. For the samples with SiV photoluminescence, their Raman spectra all exhibit high

diamond contents and low TPA contents. The graphite contents are 6.6%, 9.2%, 9.3%, and 6.0% for the samples 2.5T0, 2.5T2, 2.5T5, and 2.5T15, respectively. The sample seeded for 15 min exhibits a similar composition with the sample seeded for 5 min but with larger background noise.

The above results show that under 2.5 kPa, the particles have higher diamond content and stronger SiV PL intensity. The effects of the chamber pressure on the diamond deposition and SiV fabrication can be attributed to two factors. First, the concentration of hydrogen active groups increases with increased pressure.[31,32] The lifetime of the hydrogen active groups is much longer than that of the CH_3 active group, and the CH_3 active group is sensitive to the chamber pressure.[33] Second, the concentration of hydrogen atoms is reduced with reduced pressure.[34] Therefore, the ratio of CH_3 groups to H groups on the substrate increases with the decreased chamber pressure. In addition, the SEM graphs in Figs. 1 and 3 indicate that the shape of the synthesized diamond particles transforms from the flake-shape structure to a spherical-shape when the chamber pressure is increased to 2.5 kPa.

Comparing the PL spectra and the corresponding Raman spectra in Fig. 4(b), we find that the sample without seeding has a weak diamond peak and does not exhibit SiV photoluminescence. The photoluminescence of SiV is quenched by the high dense graphite phase.[30,35] The diamond peak positions of the 1.6 kPa and 2.5 kPa synthesized samples are slightly shifted by about 1 cm^{-1} compared with that of the ideal diamond.[36] This indicates that the synthesized diamond grains exhibit excellent quality and minimum internal stress. The samples synthesized at different pressures exhibit a similar diamond quality but different diamond contents. This is consistent with other researchers' results that the lower pressure is favorable for diamond nucleation but adverse for diamond growth.[37,38] Combining the PL spectra, Raman spectra, and SEM graphs, we conclude that diamond particles grew under 2.5 kPa chamber pressure with 2–5 min seeding time exhibit better SiV photoluminescent property.

To further investigate the effects of the pressure on the microstructure and SiV PL, we synthesized diamond particles on an optical fiber with the chamber pressure increased to 3.5 kPa and 4.5 kPa, respectively. Figure 5 displays their PL and corresponding Raman spectra. The insets are their SEM morphologies. Figure 5(a) indicates that the sample synthesized at 3.5 kPa exhibits a relatively weak SiV photoluminescence since it mainly consists of TPA and graphite with a small

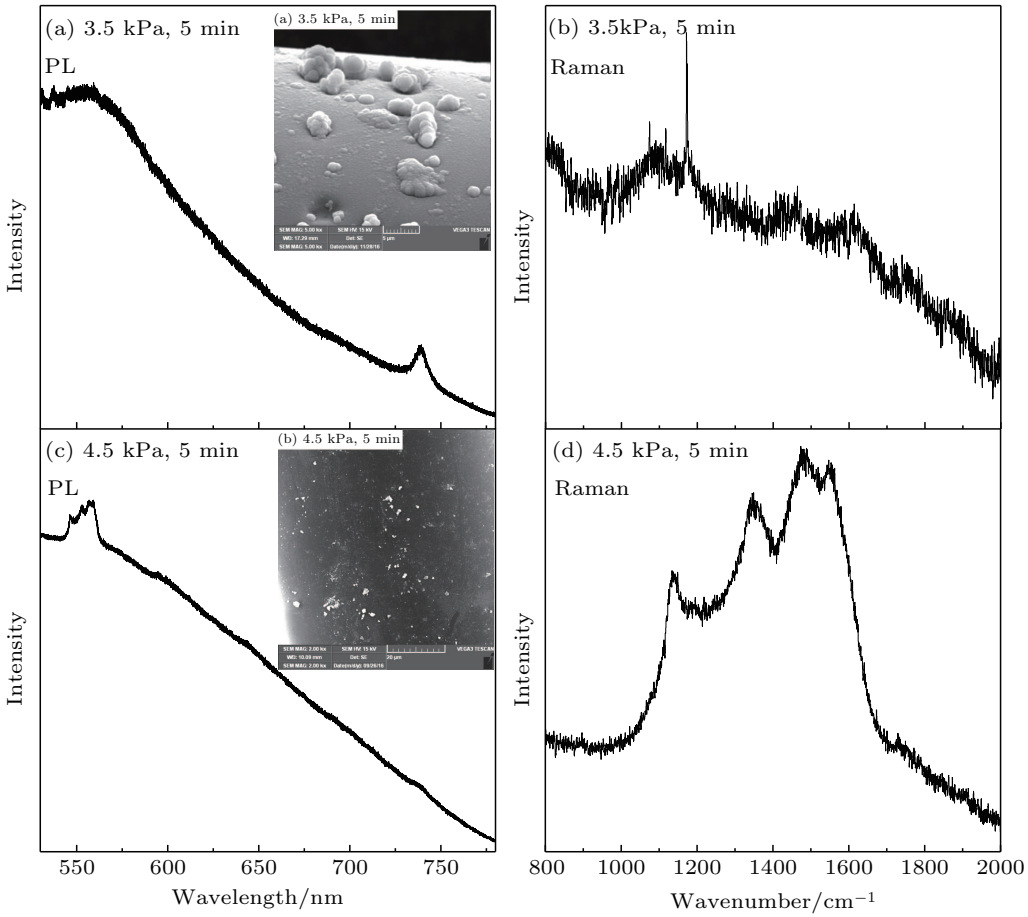


Fig. 5. The PL and Raman spectra of diamond particles synthesized under the chamber pressure of (a), (b) 3.5 kPa and (c), (d) 4.5 kPa with 5 min seeding time. Insets show the corresponding SEM graphs.

amount of diamond. Its SEM shows that spherical-shaped particles are in homogeneously distributed on the fiber surface with size around hundreds of nanometers to several micrometers. The SiV ZPL position is around 739 nm with FWHM about 8 nm. This indicates that a pressure of 3.5 kPa results in a relatively poor SiV photoluminescent property.

Figure 5(b) shows the PL, Raman spectra and SEM morphology of the samples synthesized under 4.5 kPa. The PL spectrum shows the absence of SiV photoluminescence peak. And the corresponding Raman spectrum indicates that the sample consists of non-diamond phase like TPA and graphite with few diamond contents. Some flake-shaped particles with size about 800 nm to 1 μm are observed in the samples. Comparing Figs. 5(a) and 5(b), we can conclude that a high chamber pressure of 4.5 kPa is not suitable to deposit SiV center contained diamond particle on the fiber.

Our results show that it is difficult to prepare diamond particles on the optical fiber with a single SiV center in our present study. By further adjusting the experiment parameters, like the controlled doping of silicon during diamond deposition, few SiV color centers in diamond will be obtained. Our results supply a crucial step toward the integration of optical fiber and SiV centered diamond particles.

4. Conclusion

By adjusting the deposition parameters in the CVD process, we synthesize the SiV photoluminescent diamond particles on the fiber surface. The effects of the chamber pressure on the microstructural and photoluminescent properties of the diamond particles are investigated. The results show that the samples synthesized under 2.5 kPa exhibit better SiV photoluminescent property. The particles with size around 200–400 nm are uniformly distributed on the fiber surface. With the chamber pressure increased to 3.5 kPa, the diamond quality becomes worse and non-diamond phase contents increase, weakening the SiV photoluminescent intensity. In the case of 4.5 kPa, the contents of diamond continuously decrease with increased TPA and graphite, so that the synthesized particles exhibit no SiV photoluminescence.

References

[1] Kurtsiefer C, Mayer S, Zarda P and Weinfurter H 2000 *Phys. Rev. Lett.* **85** 290

[2] Brassard G, Lütkenhaus N, Mor T and Sanders B C 2000 *Phys. Rev. Lett.* **85** 1330

[3] Claudon J, Bleuse J, Malik N S, Bazin M, Jaffrennou P, Gregersen N, Sauvan C, Lalanne P and Gérard J M 2010 *Nat. Photon.* **4** 174

[4] Dutt M V G, Childress L, Jiang L, Togan E, Maze J, Jelezko F, Zibrov A S, Hemmer P R and Lukin M D 2007 *Science* **316** 1312

[5] Jiang Q, Li W, Tang C, Chang Y, Hao T, Pan X, Ye H, Junjie Li and Gu C 2016 *Chin. Phys. B* **25** 118105

[6] Wu E, Rabeau J R, Roger G, Treussart F, Zeng H, Grangier P, Prawer S and Roch J F 2007 *New J. Phys.* **9** 434

[7] Aharonovich I, Castelletto S, Johnson B C, McCallum J C, Simpson D A, Greentree A D and Prawer S 2010 *Phys. Rev. B* **81**

[8] Babinec T M, Hausmann B J M, Khan M, Zhang Y, Maze J R, Hemmer P R and Lončar M 2010 *Nat. Nanotechnol.* **5** 195

[9] Mei Y S, Fan D, Lu S H, Shen Y G and Hu X J 2016 *J. Appl. Phys.* **120** 225107

[10] Hu X J and Li N 2013 *Chin. Phys. Lett.* **30** 088102

[11] Schröder T, Schell A W, Kewes G, Aichele T and Benson O 2011 *Nano Lett.* **11** 198

[12] Ruan Y, Gibson B C, Lau D W M, Greentree A D, Ji H, Ebendorff-Heidepriem H, Johnson B C, Ohshima T and Monro T M 2015 *Sci. Rep.* **5** 11486

[13] Rabeau J R, Huntington S T, Greentree A D and Prawer S 2005 *Appl. Phys. Lett.* **86** 134104

[14] Xu Y, Cui L, Li X, Guo C, Li Y, Xu Z, Wang L and Fang W 2016 *Chin. Phys. B* **25** 124205

[15] Qin H, Niu Y, Meng R, Lin X, Lai R, Fang W and Peng X 2014 *J. Am. Chem. Soc.* **136** 179

[16] Hepp C, Müller T, Waselowski V, Becker J N, Pingault B, Sternschulte H, Steinmüller-Nethl D, Gali A, Maze J R, Atatüre M and Becher C 2014 *Phys. Rev. Lett.* **112**

[17] Neu E, Steinmetz D, Riedrich-Möller J, Gsell S, Fischer M, Schreck M and Becher C 2011 *New J. Phys.* **13** 025012

[18] Kunuku S, Chen Y C, Yeh C J, Chang W H, Manoharan D, Leou K C and Nan L 2016 *Mater. Res. Express* **3** 106205

[19] Gruen D M 1999 *Annu. Rev. Mater. Sci.* **29** 211

[20] Lifshitz Y, Lee C H, Wu Y, Zhang W J, Bello I and Lee S T 2006 *Appl. Phys. Lett.* **88** 243114

[21] Lee H J, Jeon H and Lee W S 2012 *J. Phys. Chem. C* **116** 9180

[22] Bogdanowicz R, Sobaszek M, Ryl J, Gnyba M, Ficek M, Gołuński Ł, Bock W J, Śmietana M and Darowicki K 2015 *Diam. Relat. Mater.* **55** 52

[23] Correia M R, Monteiro T, Pereira E and Costa L C 1998 *J. Appl. Phys.* **84** 2207

[24] Huang K, Hu X J, Xu H, Shen Y G and Khomich A 2014 *Appl. Surf. Sci.* **317** 11

[25] Ferrari A C and Robertson J 2000 *Phys. Rev. B* **61** 14095

[26] Hu X J, Chen C K and Lu S H 2016 *Carbon* **98** 671

[27] Xu H, Ye H T, Coathup D, Mitrovic I Z, Weerakkody A D and Hu X J 2017 *Appl. Phys. Lett.* **110** 033102

[28] Tamor M A, Haire J A, Wu C H and Hass K C 1989 *Appl. Phys. Lett.* **54** 123

[29] Dwivedi N, Kumar S, Rawal I and Malik H K 2014 *Appl. Surf. Sci.* **300** 141

[30] Liu X, Wang G, Song X, Feng F, Zhu W, Lou L, Wang J, Wang H and Bao P 2012 *Appl. Phys. Lett.* **101** 233112

[31] Connell L L, Fleming J W, Chu H N, Vestyck D J Jr, Jensen E and Butler J E 1995 *J. Appl. Phys.* **78** 3622

[32] You M S, Hong F C N, Jeng Y R and Huang S M 2009 *Diam. Relat. Mater.* **18** 155

[33] Kobashi K, Nishimura K, Kawate Y and Horiuchi T 1988 *Phys. Rev. B* **38** 4067

[34] Sharda T, Misra D S, Avasthi D K and Mehta G K 1996 *Solid State Commun.* **98** 879

[35] Iakoubovskii K, Adriaenssens G J and Vohra Y K 2000 *J. Phys.: Condens. Matter* **12** L519

[36] Aharonovich I and Neu E 2014 *Adv. Opt. Mater.* **2** 911

[37] Das D and Singh R N 2007 *Int. Mater. Rev.* **52** 29

[38] Liang X, Wang L, Zhu H and Yang D 2007 *Surf. Coat. Technol.* **202** 261